Exp. Theo. NANOTECHNOLOGY 6 (2022) 23-27 https://doi.org/10.56053/6.1.23

Optical investigations of Ag/CeO_2 nanocomposites

T. Kim[1], J. Heon[1], Y. C. Seon[1,], Dong-Soo Kim[2], Won-Chun Oh[3]*

[1]Department of Materials Science, Korea Aerospace University, Goyang, 10540, Republic of Korea
[2] Dept. of Civil and Environmental Eng., Korea Advanced Institute of Science and Technology, South Korea
[3]Department of Advanced Materials Science & Engineering, Hanseo University, Seosan-si, Chungcheongnam-do 31962, South Korea
*) Email: ycseon@kau.ac.kr

Received 30/6/2021, *Accepted*, 30/12/2021, *Published* 15/1/2022

Silver/ceria (Ag/CeO_2) nanocomposites were pre- pared from $Ce(NO_3)_3$ $6H_2O$, $AgNO_3$, and NH_4OH with different molar ratios through a hydrothermal process, and then were completed by carrying out the precursors calcining at 750 °C for 2 h under air atmosphere. Below 1 % of Ag con- centration in Ag/CeO_2 nanocomposites, the Ag crystalline structure does not appear. XRD and TEM results show evidence of two different effects (the agglomeration and the barrier effects) governing the process of crystal growth. HR- TEM image and EDX elemental analysis of the Ag/CeO_2 nanocomposite confirmed that isolated Ag nanocrystals are dispersed in the CeO_2 matrix. The red shifts are attributed to the quantum confinement effect and the valence change of the Ce^+ ions. Ag nanoparticles can help to improve the absorption of visible light, enhancing the absorption intensity of Ag/CeO_2 nanocomposite. These results are of great significance for the control of microstructure, crystallinity, and applications for the development of nanocomposite materials.

Keywords: Oxides; Optical; Composite.

1. INTRODUCTION

Nanocomposite materials show many special physical and chemical properties [1]. The Ag/CeO_2 nanocomposite attracted the attention of many experts and scholars because of the two elements of an Ag/CeO_2 system; the CeO_2 has a high oxygen storage capacity and anti-ultraviolet ray ability [2], which is applied in many areas, such as a polishing agent [3], catalyst [4], ultraviolet (UV) resistant [5], or gas sensors [6]. The other element is Ag, nanoparticles of Ag have been the key to many

important applications in catalysis [7] and optics [8]. Ag nanoparticles can also be used as an antimicrobial agent in various biomedical applications [9]. In addition, Ag is attractive for industrial applications due to its low cost and easy preparation.

Ag/CeO_2 nanocomposites are synthesized, besides having a two-element respective nature, and also extend the unique properties of composite materials to improve on its efficiency in optical, electrical, and chemical reactions. So, many techniques have been proposed for the synthesis of nanosized Ag/CeO_2 nanocomposite with promising control of properties, such as the coprecipitation method [10], the combustion method [7, 11], the impregnation method [12], the photochemical approach [13], the deposition precipitation method [14], the hydrothermal process [15], and the wet impregnation technique [16]. Synthesis of nanocomposite materials can be accomplished in a variety of ways, each method having favorable conditions and specificity. When using the hydrothermal process to synthesize nanocomposite powder, the main superiorities are simplicity of operation, low cost, good crystalline, ease of control, and the high reproducibility. Ag/CeO_2 has been reported for use as catalyst and in solid-oxide fuel cells [11, 14], but for the Ag content of Ag/CeO_2, their nanocomposite structure and op- tical properties are rarely discussed.

The study of nanocomposite material has been of great interest from both fundamental and practical point of view. The physical properties of such nanocomposite materials can be combined to produce material of desired response. In order to further improve the properties of CeO_2, various Ag concentrations in the molar ratio range of 0–10 % on CeO_2 were used to synthesize Ag/CeO_2 nanocomposite was re- ported. The aim of this present work is to study the morphology and crystal structure of compositionally homogeneous Ag/CeO_2 nanocomposite synthesized by the hydrothermal method. The optical properties of the samples were also investigated.

2. EXPERIMENTAL

Cerium nitrate hexahydrate ($Ce(NO_3)_3{\cdot}6H_2O$, 99.5 %, Aldrich Chemicals, USA), silver nitric ($AgNO_3$), nitric acid (HNO_3), polyethylene glycol (PEG 600), ammo- nia (NH_4OH), methylene blue (MB), anhydrous ethanol (99.9 %, Fisher Chemicals), distilled water and alcohol, all at analytical grades. The Ag/CeO_2 nanocomposites were prepared by the hydrothermal method. We mixed aqueous solutions of $Ce(NO_3)_3\ 6H_2O$ and $AgNO_3$ together with different molar ratios, stirred about 30 min and then slowly dropped about 25 ml of NH_4OH and 30 ml of PEG into the mixed solutions, respectively. The pH values were adjusted to 7.0, the above mixtures were poured into Teflon-lined stainless-steel autoclaves after vigorously stirring for about 2 h, and the autoclaves were maintained at 180 °C for 4 h, then air cooled to room temperature. The resultant precipitates were collected by centrifugation and washed with dis-tilled water and anhydrous alcohol three times. After these treatments, the resulting mixture was loaded into the oven at 80 °C for one day to gain precursors. At last, the precursors were calcined at 750 °C for 2 h to obtain Ag/CeO_2 nanocomposites. To determine the crystallite sizes and phases of the Ag/CeO_2 nanocomposites, the powders were identified by X-ray diffraction (XRD, Rigaku D/max-IV) using CuKα radiation (wavelength 1.5406 Å). The operation voltage and current were maintained at 40 kV and 20 mA, respectively. A scan rate of 2°/min was applied to record the patterns in the 2θ range of 25–65°. Transmission electron microscope (TEM) and selected area electron diffraction (SAED) images were obtained on a (JEOL-2100) microscope with an accelerating voltage of 200 kV. The samples were dispersed in ethanol by ultrasonic treatment for about 30 min and then the suspension was dripped onto a copper grid for TEM. Semiquantitative microprobe analysis was performed with scanning electron microscopy (SEM, JEOL JSM-6500FE). Raman microspectroscopy, based on scattering, (ULVAC, laser 633 nm) was used to characterize the surface defects of samples. The UV–Vis diffuse reflectance spectra (UV– Vis DRS) was recorded in air at room temperature in the wavelength range

of 250–800 nm using a spectrophotometer (JASCO, V-760 Diffuse Reflectance Model).

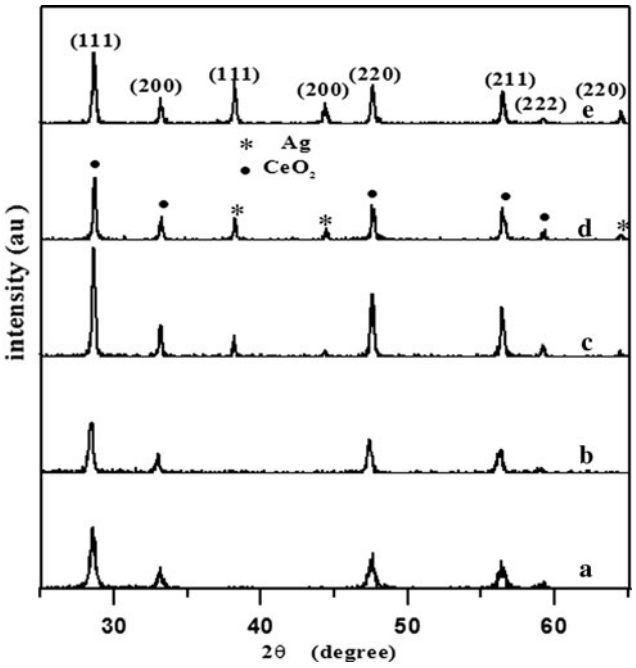

Figure 1 XRD patterns of (**a**) pure CeO_2, (**b**) 1 % Ag/CeO_2, (**c**) 2.5 % Ag/CeO2, (**d**) 5 % Ag/CeO2 , (**e**) 10 % Ag/CeO2.

3. RESULTS AND DISCUSSION

Figure 1 shows the XRD patterns of pure CeO_2 and various molar ratios of Ag/CeO_2 nanocomposites produced by hydrothermal interaction. When the Ag concentration is lower than 1 %, only the cubic structure of CeO_2 appears in the XRD analysis because the Ag content is very low. All peaks demonstrated that the main body is CeO_2, with peak position of approximately 2θ 28.54°, 33.07°, 47.48°, 56.33°, and 59.08°, corresponding to a crystalline phase of (111), (200), (220), (211), and (222), respectively; it is a face- centered cubic fluorite structure (JCPDS File No. 81-0792). The Ag concentration is lower than 1 %; only the cubic structure of CeO_2 appears in the XRD pattern. When the Ag concentration rises up to 2.5 %, the Ag crystalline phase begins to appear, metal Ag with a face-centered cubic phase structure (JCPDS File No. 89-3722) was clearly observed, (111), (200), and (220) with the corresponding 2θ values of 38.12°, 44.31°, and 64.46°, respectively. The as-products size was estimated from line broadening of CeO_2 (111) peak using Scherrer's equation [17]:

$$D = k\lambda/(\beta \cos\theta) \quad (1)$$

where D the average size of the crystallites, k Scherrer constant (0.98), λ the wavelength of radiation, β the peak width at half-height and θ the value of the diffracted angle. By fitting various peaks of the profiles to this formula, we obtained values in the range of 30 46 nm for the particle diameter.

The results are listed in Table 1. From those results, we distinguish three domains for Ag/CeO_2 nanocomposites, corresponding to three modes of the CeO_2 crystal size change. The first domain corresponds to the Ag adding con- centration between 0 and 2.5 %. In this domain, the CeO_2 mean crystallite size increases linearly with the Ag adding concentration, because of the agglomerate effects more than the barrier effect. The second domain corresponds to the Ag adding concentration between 2.5 and 5 %. In this domain, the increasing of the CeO_2 crystallite size becomes less pronounced, both agglomeration and barrier effect on growth trend to balance. The third domain corresponds to the Ag adding concentration between 5 and 10 %. In this domain, the CeO_2 mean crystallite size decreases with the Ag adding concentration, the main reason is the Ag barrier affect the crystal growth, and led to the grain size reduction. The lattice parameters have changed with the adding Ag contents.

4. CONCLUSIONS

Ag/CeO_2 nanocomposites can be successfully synthesized by a hydrothermal method with different molar ratio con- centrations (0∼10 %) of Ag. XRD and SAED indicated that the particles of the Ag/CeO_2 were well crystalline, and HR-TEM as well as EDX elemental analysis proved the formation of nanocomposite between CeO_2 and Ag. Adding Ag will affect the structures and optical properties of Ag/CeO_2 nanocomposites. The agglomeration effect and the barrier effect governing the process of crystal growth. The crys- tal growth of agglomerated CeO_2 is faster than pure CeO_2 through high temperature heat treatment. The absorption in- tensity of Ag/CeO_2 nanocomposite increases in the visible region as the amount of Ag increases.

References

[1] A.P. Alivisatos, Science 271 (1996) 933
[2] X.L. Zhang, K.J. Klabunde, Inorg. Chem. 31 (1992) 1706
[3] V.D. Kosynkin, A.A. Arzgatkina, E.N. Ivanov, M.G. Chtoutsa, A.I. Grabko, A.V. Kardapolov, N.A. Sysina, J. Alloys Compd. 303 (2000) 421
[4] Liqaa H. Alwaan, Layla A. Jubur, Doaa A. Hussein, Exp. Theo. NANOTECHNOLOGY 4 (2020) 35
[5] S. Tsunekawa, T. Fukuda, A. Kasuya, J. Appl. Phys. 87 (2000) 1318
[6] T.S. Stefanik, H.L. Tuller, J. Eur. Ceram. Soc. 21 (2001) 1967
[7] P.R. Sarode, K.R. Priolkar, P. Bera, M.S. Hegde, S. Emura, R. Ku- mashiro, Mater. Res. Bull. 37 (2002) 1679
[8] I.A. Wani, A. Ganguly, J. Ahmed, T. Ahmad, Mater. Lett. 65 (2011) 520
[9] M. Strathmann, J. Wingender, Int. J. Antimicrob. Agents 24 (2004) 234
[10] S. Imamura, H. Yamada, K. Utani, Appl. Catal. A, Gen. 192 (2000) 221
[11] P. Bera, K.C. Patil, M.S. Hegde, Phys. Chem. Chem. Phys. 2 (2000) 3715
[12] Halima Mazari, Kheira Ameur, Aicha Boumesjed, Reski Khelifi, Sedik Mansouri, Nadia Benseddik, Nawal Benyahya, Zineb Benamara, Jean-Marie Bluet, Exp. Theo. NANOTECHNOLOGY 4 (2020) 49
[13] S. Scire, C. Crisafulli, S. Giuffrida, C. Mazza, P.M. Riccobene, A. Pistone, G. Ventimiglia, C. Bongiorno, C. Spinella, Appl. Catal. A, Gen. 367 (2009) 138
[14] J.H. Wang, M.L. Liu, M.C. Lin, Solid State Ion. 177 (2006) 939
[15] Bassam Ramadhn Sarheed, Muhammed Abdul gafor, Mustafa. R. Al-Shaheen, Mohammed R. Alshaheen, Exp. Theo. NANOTECHNOLOGY 4 (2020) 59
[16] M. Itome, A.E. Nelson, Catal. Lett. 106 (2006) 21

[17] B.D. Cullity, S.R. Stock, Elements of X-Ray Diffraction Prentice Hall, Upper Saddle River (2001)